A Hybrid Discrete-Continuum Model for 3-D Skeletogenesis of the Vertebrate Limb

R. Chaturvedi[1], C. Huang[2], J.A. Izaguirre[2], S.A. Newman[3], J.A. Glazier[4], and M. Alber[1*]

[*]Author for correspondence: malber@nd.edu.
[1]Department of Mathematics, University of Notre Dame, Notre Dame, IN 46556.
[2] Department of Computer Science and Engineering, University of Notre Dame, Notre Dame, IN 46556-5670.
[3]Department of Cell Biology & Anatomy, New York Medical College, Vallaha, NY
[4] Biocomplexity Institute and Department of Physics, Indiana University, 727 East 3rd Street, Swain Hall West 159, Bloomington, IN 47405-7105.

Abstract. We present a dynamic, three-dimensional, composite model framework for vertebrate development. Our integrated model combines submodels that address length-scales from subcellular to tissues and organs in a unified framework. Interacting submodels include a discrete model derived from non-equilibrium statistical mechanics (Cellular Potts Model) and continuous reaction-diffusion models. A state diagram with associated rules and a set of ordinary differential equations model genetic regulation to define and control cell differentiation. We apply the model spatiotemporal bone patterning in the *proximo-distal* (from body towards digits) direction of developing avian limb.

1 Introduction

The volume of information modern molecular biology provides on genetics and biochemistry can obscure dynamical processes underlying the generation and function of complex biological phenomena. Predictive models and simulations can aid our understanding of such phenomena, particularly if they take into account experimentally-determined cellular and molecular details and treat the complex interactions between various natural scales of biological objects and processes.

In previous papers [1, 2] we described a systems-biology approach to integrating *discrete* and *continuous* models of biological developmental mechanisms to build a reduced, 2-dimensional (*2D*) model of vertebrate limb development. We used *discrete* models to describe cell movement and division, interactions between individual cells, and *differentiation* (changing of fundamental sets of behaviors by turning on or off clusters of genes) from multipotent cells into specific cell types, and continuous models to describe extracellular signaling molecules. Simulations reproduced the proximodistal increase in the number of skeletal elements over time in the developing limb. This paper presents a 3-dimensional (*3D*) multiscale framework for modeling *morphogenesis* (structural development of an organism or its organs) during embryonic development in vertebrates. At subcellular and molecular scales,

P.M.A. Sloot, B. Chopard, and A.G. Hoekstra (Eds.): ACRI 2004, LNCS 3305, pp. 543–552, 2004.

morphogenetic molecules are secreted, diffuse and interact. At the scale of cells, morphogenesis involves cell growth, proliferation, differentiation, migration and death. At larger scales, bulk changes in the shapes of tissues produce the dramatic patterns of tissues and organs. We develop submodels for this hierarchy of scales, and combine them into an integrated multiscale model. Specific differences from the 2D model are detailed when dealing with submodels. While 2D simulations can serve as a guide to model building, an adequate understanding of 3D biological phenomena can only be achieved with 3D simulations.

Genes specify products necessary for morphogenesis, but not their distribution or physical effects. Generic physical mechanisms (mechanisms common to living and nonliving materials) organize the materials the genetic mechanisms provide [3]. Experiments on initiation and arrangement of individual skeletal elements in chicken and mouse embryos suggest that the secreted morphogens TGF-β, FGF-2 and FGF-8 are key molecules of a core patterning process, as is the extracellular matrix (ECM) adhesive protein *fibronectin* (reviewed in [4]). Cells differentiate from multipotent stem cells into specialized cell types of the developed organism. Cells diversify into distinct *differentiation types* during development. Differentiation from one cell type to another is a comprehensive qualitative change in cell behavior, generally irreversible and abrupt (*e.g.*, responding to new sets of signals, turning on or off whole genetic pathways). Cells of the same type can exist in different states; but different states typically differ less in their behavior than cells of two different types. The concept of cell types is used to model the major behavioral groups of cells.

Our earlier 2D model for spatiotemporal regulation of *chondrogenesis* (cartilage development) of the vertebrate limb reproduced the biological generation of a sequence of increasing numbers of parallel cartilage elements in proximo-distal sequence (for figures, see [1]). In an avian (chicken) forelimb, the numbers and identities of the main elements are 1 (humerus), 2 (radius+ulna) and 3 (digits). Bones at different proximo-distal levels differ in size and shape (*e.g.*, the humerus is longer and thicker than the ulna). Differences between elements (*e.g.*, different fingers) in the anterior-posterior direction are subtler. Bone replaces the cartilage elements later in development.

Organogenesis depends on the 3D rearrangement of cells. Although 2D simulations provide helpful qualitative insights and require less computing time to run, symmetries and symmetry-breaking during organogenesis differ qualitatively in 3D. This paper treats issues specific to 3D and describes both normal and pathological limb development. Our model framework for organogenesis includes three major submodels: the discrete stochastic Cellular Potts Model (CPM) for cell dynamics, continuum reaction-diffusion (RD) partial differential equations (PDEs) for morphogen production and diffusion, and a state automaton for cell type transition (TT) to model differentiation. The extra degree of translational freedom in 3D CPM relaxes 2D constraints on producing specific structures (*e.g.*, cylindrical condensations of cells in real chondrogenesis). In organisms, patterns of diffusing morphogens, which serve both as *inductive* signals (altering cell type) and *chemotactic* signals (inducing cell movement along chemical gradients), must be stable for time scales of interest. Our earlier 2D simulations [1] used the Schnakenberg RD equations (see [5]) as a specific continuum RD example. We introduced additional cubic terms modifying cells' morphogen production based on our analysis of bifurcations of the Schnakenberg equations in 3D. Parameters associated with these terms also make 3D equations structurally more complex.

2 Biological Background: Multiple Scales in Organogenesis

Hentschel *et al.* [4] outline the biological basis of the model of chicken limb development considered here (see also [1] and [2]). An initial tissue mass, the paddle-shaped *mesoblast*, contains pre-differentiated mesenchymal cells. During successive stages of chondrogenic patterning in the chick limb, cells divide and cluster (condense) at increasingly distal locations and differentiate into chondrocytes, forming the cartilage template for limb skeleton. We consider two main secreted components--the morphogen TGF-β and the ECM molecule fibronectin. The former diffuses through mesoblast; the latter is a larger molecule that accumulates at secretion sites. We assume that the bulk of the ECM provides a medium for diffusion of TGF-β and a hypothesized inhibitor of TGF-β production, action or the action of its downstream effectors [6; 7], and for fibronectin accumulation. Cells diffuse and undergo hatptotaxis in response to fibronectin, *i.e.*, they move up gradients of fibronectin. TGF-β diffuses through the mesoblast and is positively autoregulatory [6]. TGF-β also induces cells to produce fibronectin and upregulates cell-cell adhesivity [8], which recruits neighboring cells into chondrogenic condensations. We make the simplifying assumption that the fibronectin signal upregulates cell-cell adhesion, thus reinforcing accumulation of cells at high fibronectin zones. The three zones in a developing limb are- *apical* where cells only divide; *active* where cells rearrange locally into precartilage condensations; and *frozen* where condensations have differentiated into cartilage and patterning ceases. Cell division continues in both active and frozen zones. Certain FGFs emanating from the apical ectodermal ridge (AER) a band of cells along the anteroposterior margin at the tip of the limb bud have concentration-dependent effects on the underlying cells and thus define the zones [4]. For simplicity, we assume the zones *a priori*.

3 Physical and Mathematical Submodels and Their Integration

Modeling Cellular and Tissue Scales: The CPM Framework

Cell-scale processes underpin the complexity of multicellular organisms. The simplest cell-cell interaction is adhesion, which allows cells to form stable clumps and, combined with cell motility, allows different types of cell with different adhesivity to sort into clusters of like type [9]. Differences in adhesivity result from differences in the quantity and identity of cell adhesion molecules (CAMs) on cell membranes. Modeling variations in cell-specific adhesivity, rather than modeling individual CAMs, suffices to explain cell sorting and clustering in experiments. CPM, our *framework* for modeling cells and their dynamics, describes cell behaviors using an effective energy, E, comprised of real (*e.g.*, cell-cell adhesion) and effective (*e.g.*, the response of a cell to a chemotactic gradient) energies and constraints [10]. CPM dynamics uses imposed fluctuations and strong dissipation to rearrange cell configuration to minimize E. E includes terms to model (i) haptotaxis (ii) variations in cell adhesivity (iii) cell growth, and (iv) division (*mitosis*). CPM uses a lattice to describe cells. Each lattice site (*voxel*) has an associated integer index (*spin*). Value of index at a lattice site is σ if the site lies in cell σ. *Domains* (collections of lattice sites with the same index) represent cells. A cell is thus a set of discrete components that can rearrange, resulting in cell shape changes and motions. A voxel interacts locally

with voxels within an *interaction range*. Each cell has an associated type. ECM is modeled as a generalized cell of distinct type. In [11], quantitative justification of the CPM is provided.

CPM is an efficient and convenient phenomenological framework for modeling the behavior of groups of cells. It uses a minimal number of parameters which have clear physical meanings. Models using molecular-scale chemical reaction-kinetics or intermediate scales (*e.g.* at the level of the cytoskeleton or membrane) are feasible for at most a few cells. M-Cell and VirtualCell[1] are successful examples of such detailed models. In our simulations, where tens or hundreds of thousands of cells differentiate and organize into tissues, completely microscopic approaches are computationally exorbitant and unnecessary. We do introduce micro-scale modeling of mechanisms when appropriate.

The phenomenological parameter T, an *effective temperature*, drives cell-membrane fluctuations. Fluctuations follow the Metropolis algorithm for Monte-Carlo Boltzmann dynamics. A proposed change in lattice configuration produces a change in effective energy, ΔE. We accept it with probability:

$$P(\Delta E) = 1, \Delta E \le 0; \qquad P(\Delta E) = e^{-\Delta E / kT}, \Delta E > 0, \tag{1}$$

where k is a constant converting T into units of energy and E includes terms to describe each mechanism we wish to model, *e.g.*,

$$E = E_{contact} + E_{volume} + E_{chemical}, \tag{2}$$

$E_{contact}$ describes the net adhesion/repulsion between two cell membranes.

$$E_{contact} = \sum_{(i,j,k)(i',j',k')} J_{\tau(\sigma)\tau'(\sigma')}(1-\delta(\sigma(i,j,k),\sigma'(i',j',k'))), \tag{3}$$

$J_{\tau\tau'}$, the binding energy per unit area depends on types of interacting cells, τ and τ'. *Kronecker delta*, $\delta(\sigma,\sigma')=0$ if $\sigma \neq \sigma'$ and $\delta(\sigma,\sigma')=1$ if $\sigma=\sigma'$. Sum is over the interaction range.

A cell of type τ has a prescribed target volume $v(\sigma,\tau)$ and surface area $s(\sigma,\tau)$. The actual volume and surface area fluctuate due to changes in osmotic pressure, pseudopodal motion of cells, *etc*. Changes also result from the growth and division of cells. E_{volume} enforces these targets by exacting an energy penalty for deviations. E_{volume} depends on four model parameters: *volume elasticity*, λ, *target volume*, $v_{target}(\sigma,\tau)$, *membrane elasticity*, λ', and *target surface area*, $s_{target}(\sigma,\tau)$:

$$E_{volume} = \sum_{all-cells} \lambda_\sigma (v(\sigma,\tau) - v_{target}(\sigma,\tau))^2 + \sum_{all-cells} \lambda'_\sigma (s(\sigma,\tau) - s_{target}(\sigma,\tau))^2. \tag{4}$$

Cell Growth and Division: Cell growth results when $v_{target}(\sigma,\tau)$ and $s_{target}(\sigma,\tau)$ increase with an increasing number of *CPM steps* (time). We model cell division by starting with a cell of average size, $v_{target} = v_{target,average}$, causing it to grow by gradually increasing v_{target} to $2v_{target,average}$, and splitting the cell into two cells, each with a new target volume: $v_{target}/2$. One daughter cell assumes a new σ. A modified breadth-first search selects

[1] http://www.mcell.cnl.salk.edu/, and http://www.life.uiuc.edu/plantbio/cell/

the voxels which receive the new spin; the split is approximately along the cell diameter. For cell death we set the cell's target volume to zero.

Cells can respond to chemical signals by moving along concentration gradients. A chemotaxis/haptotaxis model requires a description of the evolving, spatially-varying chemical *concentration field* for each chemical, and an *interface* to connect the field to the CPM framework for cell and tissue dynamics. $C(\vec{x})$ is the local concentration of the molecule. An effective chemical potential, $\mu(\sigma)$ translates the effect of the chemical on cell motion into the CPM energy formalism. We use the simplest possible form of this coupling:

$$E_{chemical} = \mu(\sigma)C(\vec{x}). \tag{5}$$

In the above, $\vec{x}$ is the position vector; when we match the grid to the (i,j,k) in the CPM model we approximate it to the voxel it lies in.

Modeling Molecular Scales: Reaction-Diffusion Equations

In [12], Turing introduced the idea that interactions of reacting and diffusing chemicals (at least one autocatalytic *activator* species and one *inhibitor* species which represses the activator) could produce self-organizing instabilities that might explain biological patterning. To model the behavior of TGF-β in the limb, we use RD and chemotactic coupling to the cells, but no back-coupling from the cells to the chemical field [5; 4]. Thus, the response of cells to TGF-β depends on the RD *pre-pattern* of TGF-β. Assuming isotropic diffusion:

$$\frac{\partial u}{\partial t} = D\,\nabla^2 u + \gamma F(u), \tag{6}$$

where $u=(u_1,u_2)^T$ and $D=diag(d_1,d_2)$, u_1 is an activator (TGF-β in the chicken limb) and u_2 is a hypothetical inhibitor [6; 7].

We are also working on removing the above simplification of having no back-coupling (equivalent to assuming a non-biological source term in the RD equations), see "Work In Progress" below. The modified RD equations include this back coupling and the resulting feedback from cells.

The 2D model in [1] used the Schnakenberg equations, *i.e.*, $F=(F_1,F_2)^T$ with $F_1=a-u_1+u_1^2u_2$ and $F_2=b-u_1^2u_2$. Here, for the *growing* limb bud we seek 3D solutions cylindrically elongated in z (distal) direction. For these patterns to be stable in 3D, we needed to circumvent the observation that stability of stripes and spots is mutually exclusive for the Schnakenberg equations (see [13]). Accordingly, we modified the forms of F_1 and F_2 [13] to:

$$\begin{aligned} F_1 &= a - u_1 + u_1^2 u_2 + \mathrm{k}_1(u_1 - u_{01})^3 \\ F_2 &= b - u_1^2 u_2 + \mathrm{k}_2(u_2 - u_{02})^3. \end{aligned} \tag{7}$$

The cubic terms do not change the behavior in an essential way as long as u is close to u_0, where u_0 is a stable solution of $F(u)=0$. Thus, Equation 6 becomes:

$$\frac{\partial u}{\partial t} = \gamma(a - u + u^2 v + k_1(u - u_*)^3) + (D_x \frac{\partial^2 u}{\partial x^2} + D_y \frac{\partial^2 u}{\partial y^2} + \frac{\partial^2 u}{\partial z^2}), \quad (8)$$

$$\frac{\partial v}{\partial t} = \gamma(b - u^2 v + k_2(v - v_*)^3) + d(D_x \frac{\partial^2 v}{\partial x^2} + D_y \frac{\partial^2 v}{\partial y^2} + \frac{\partial^2 v}{\partial z^2}).$$

We solved Equations 8 using an explicit finite-difference scheme over a rectangular domain. Separately, or in combination, the set of parameters γ (relative strength of production vs. diffusion), the ratio l_x/l_y and diffusion coefficients of activator and inhibitor control the number of cylinders and their geometry (mathematically, these changes are equivalent). For instance, decreasing the diffusion coefficient (which is mathematically equivalent to changing the aspect ratio of the domain) in the *x*-direction by a factor of m^2 increases the number of spots in the *x*-direction by a factor of *m*. We use the no-flux boundary conditions. Field values are initialized to a uniform distribution perturbed randomly by a small value.

Modeling Macromolecular Scales: Fibronectin

We assume that cells respond to the TGF-β signal by producing a substratum adhesion molecule (SAM), which we identify with fibronectin, and CAM, which we identify with N-cadherin. We treat fibronectin as a non-diffusing chemical field, which results in slower computations, but is simpler than treating it as a generalized cell within the CPM framework. Cells undergo haptotaxis in the direction of increasing SAM [14]. In addition, the fibronectin signal upregulates cell-cell adhesion, which enhances the accumulation of cells. Hence cells tend to cluster in regions of high fibronectin concentration and reinforce this tendency by secreting more fibronectin within those regions.

Although the Turing-instability-generated TGF-β prepattern initiates fibronectin patterning, self-enhancing *positive feedback* of SAM secretion and CAM upregulation consolidates subsequent patterning. Our model represents an extension of the original CPM introduced by [10] insofar as we introduce a SAM term governing cell haptotaxis (Equation 5), and we allow the strength of CAM-dependent interaction to vary based on morphogen concentration (Equation 3).

Cell Types and the Type Transition Model

All cells of a particular differentiation type share a set of parameters describing their state, while two different cell types (*e.g.*, muscle and bone) have different parameter sets. Cells of the same type exist in different states, corresponding to a specific set of values for the cell-type's parameters. A cell's behavior depends on its state. Genetic and external cues influence both cells' type and state. We model differentiation using a *Type Transition Model* (TT). Each type in this model corresponds to a cell differentiation type (with a defined parameter set) that exists during limb chondrogenesis. Change of a cell from one type to another corresponds to cell differentiation. The type-change map models regulatory networks by defining the rules governing type change, *e.g.*, accounting for the intra- and inter-cellular effects of chemical fields. In the avian limb, one cell type of interest is the initial *precartilage mesenchymal* cell, which can translocate, divide, and produce various morphogens and ECM molecules. All cell types in chick limb undergo mitosis. We assume that

cells in the active zone represent a cell type distinct from those in the apical zone. Specifically, unlike the apical zone cells, *active zone cells* respond to activator, inhibitor, and fibronectin. When a responsive cell in the active zone senses a threshold local concentration of activator, its type changes to *fibronectin-producing*. A fibronectin-producing cell can upregulate its cell-cell adhesion (the parameter $J_{\text{cell,cell}}$ in the CPM decreases). Cells that have not experienced local threshold levels of activator can respond to, but not produce, fibronectin. This model of genetic regulation captures the formal, qualitative aspects of regulatory interactions (reviewed in [15] and [4]).

The Scale of the Organ: Integration of Submodels

We must integrate the CPM (stochastic, discrete), RD (continuum, PDEs) and TT (rule based state automaton) submodels while maintaining their modularity, *e.g.* by: (i) Matching the spatial grid for the continuum and stochastic models and (ii) Defining the relative number of iterations for RD and CPM evolvers. The SAM and CAM submodels form a positive feedback loop (of SAM secretion and CAM upregulation) providing the *biologically-motivated* interface between the RD-based TGF-β prepattern and the CPM-based cell dynamics. The RD engine uses an explicit solver, based on forward time marching. We store these calculations as *fields*, *e.g.,* the TGF-β concentration. The CPM simulator implements the lattice abstraction and the Monte Carlo procedure. Acceptance probability function is Metropolis by default. We can view the CPM as an operation on a field of voxels. Various fields can evolve under their own set of rules—Metropolis dynamics for the field of voxels, RD for the field of morphogens. A chemical like fibronectin, which cells secrete and which then remains in place, is another concentration field, the corresponding evolver rule is reaction dynamics with no diffusion. A description of genetically determined response of the cells controls the TT evolver governing cell differentiation. Other sub-modules implement different cell responses, *e.g.*, cell growth and mitosis. Criteria for interfacing the various grids and time scales specify the simulation protocol. In the simulations we present in this paper, we keep the CPM and RD grids identical, but the software framework can also handle different sized rectangular grids. The CompuCell web site[2], distributes the Open Source software.

4 Brief Discussion of Simulation Results

The combined behavior of morphogens, cell dynamics and cell differentiation results in a biologically realistic, roughly periodic pattern of the major chondrogenic elements. The model demonstrates global emergent phenomena resulting from local interactions as well as nonlocal coupling. Sources of nonlocal coupling are present in both the RD and CPM submodels. While reaction is local, diffusion introduces a nonlocal interaction on the scale of the diffusion length and limited to the domain of the diffusion. CPM is non-local because of the volume and area constraints, which connect sites across a cell diameter. However, the emergent pattern of bones has structures much larger than the RD and CPM interaction lengths. We first present the *normal* pattern of precartilage condensation in the chick forelimb: one followed by

[2] http://www.nd.edu/~lcls/compucell

two and then three primary (*i.e.*, excluding the wrist bones) elements successively in the proximodistal direction. The SAM concentration and cell condensation patterns follow the activator prepattern. Figure 1 shows simulations of the full 3D chick-limb chondrogenesis model, where the cells have condensed into the chondrogenic pattern of a chick forelimb.

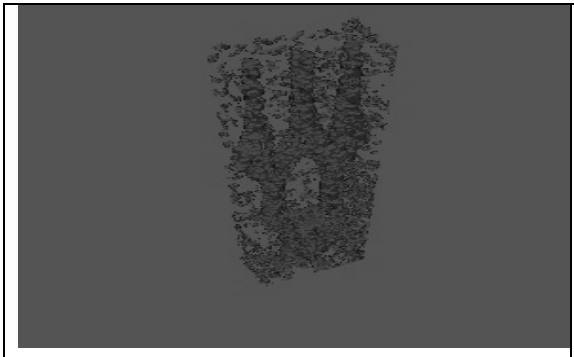

Fig. 1. Normal development of chondrogenic condensations: Cell con-densation into humerus, ulna +radius, and digits in 3D simulation.

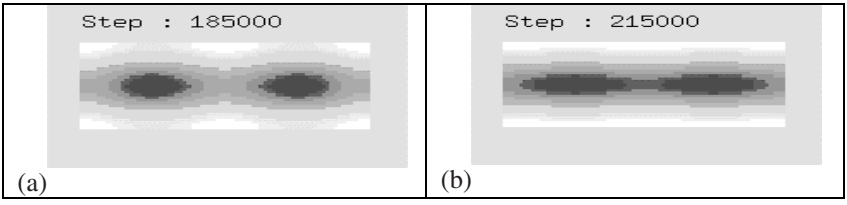

Fig. 2. (a) and (b) show transverse sections of TGF-β concentration, with no cubic stabilizing term for activator (k_1=0, k_2=0.375). Stripes rather than spots are stable, corresponding to fused digits (Apert Syndrome).

We also study the effect of parameter changes affecting the cubic terms describing the production of the activator and inhibitor and relate it to both normal and abnormal growth. The relative effect of the activator and inhibitor cubic terms is of interest. Figures 2 (a) and (b) show TGF-β concentrations in transverse sections of the simulated chick limb in the distal region at successive times , for k_1=0 (no cubic term for the activator). Patterning in the proximal region proceeds normally, up to the bifurcation of the solution into two cylindrical elements (two spots in cross-section). As time progresses, the two elements fuse into one long stripe in the transverse section, equivalent to the pathology of fused elements (Apert syndrome in humans [16]). The results were similar for small positive values of k, $0<k_1\approx k_2<0.1$. Figure 3 shows results for k_2=0 (no cubic term for the inhibitor). The normal pattern of bone elements is seen. Thus the activator cubic term suffices to stabilize the spots in transverse section. We can interpret the four intermediate spots in Figure 3 as carpal (i.e., wrist) bones.

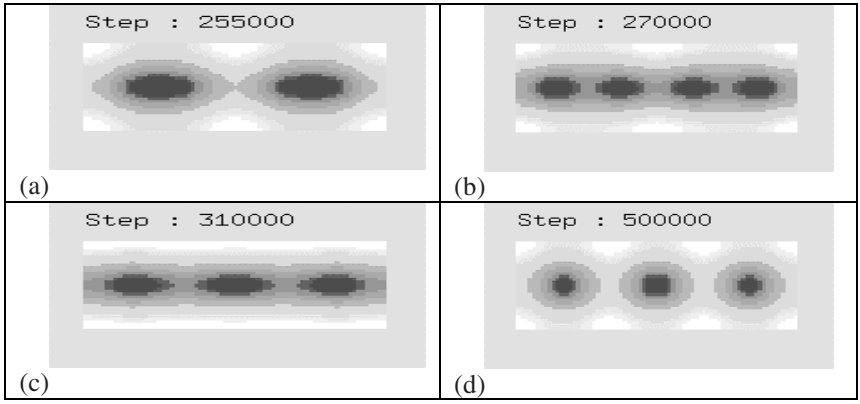

Fig. 3. Transverse sections of TGF-β concentration with no cubic stabilizing term for inhibitor (k_2=0, k_1=0.125). We obtain the normal pattern, indicating that the activator's cubic stabilization is crucial for generating the bone element pattern. The intermediate stage of four spots resembles the many carpal bone elements.

In summary, normal-looking patterns of the major chondrogenic elements were obtained for a relatively robust range of parameter changes. The correct stable pattern, especially the formation of distinct digits, requires the cubic terms in the equations describing the production of activator and inhibitor, with the activator cubic term more important. This may be justified, in part, by results described in [13] and references therein, showing this to be a general result for the kind of RD systems we consider- i.e., with only the first order terms for reactions, it is not possible to get both "stripes" and "spots" in a stable pattern. Other forms may stabilize the solution; for example, the assumption that fibronectin diffuses a short distance stabilizes [17] the biologically-motivated system of equations for skeletal development studied in [4]. These possibilities can motivate experimentation to determine whether this class of models is viable and if so, how stabilization is actually achieved.

Work in progress: We are extending the model to make the production of TGF-β as realistic as that of fibronectin, to include secretion at cell boundaries, rather than modeling secretion at the domain level. We will incorporate and extend the work of [4], which uses a continuum model of interaction between limb cells and gene products to obtain a more realistic set of RD equations. We are extending our simulation geometry module to incorporate the limb domain's moving boundaries. To incorporate the AER we are introducing two additional cell types, both *epithelial* (cells that cover the outer surface of the limb and give rise to skin) apical epithelial cells which secrete a mixture of FGFs characteristic of the AER, and epithelial cells that secrete a different mixture of FGFs [18].

Acknowledgements. We acknowledge support from NSF grants IBN-0083653, IBN-0090499, and ACI-0135195, NASA grant NAG 2-1619, an IBM Innovation Institute Award and a IUB Pervasive Technologies Laboratories Fellowship.

References

1. Chaturvedi, R., Izaguirre, J. A., Huang, C., Cickovski, T., Virtue, P, Thomas, G., Forgacs, G., Alber, M., Hentschel, G., Newman, S. A., and Glazier, J. A., Computational Science - ICCS 2003: International Conference Melbourne, Australia and St. Petersburg, Russia, June 2-4, 2003. Proceedings, Part III, P. M. A.Sloot, D. Abramson, A. V. Bogdanov, J. J. Dongarra, A. Y. Zomaya and Y. E. Gorbachev editors (LNCS Volume 2659, Springer-Verlag, New York), (2003) 39-49.
2. Izaguirre, J. A., Chaturvedi, R., Huang, C., Cickovski, T., Coffland, J., Thomas, G., Forgacs, G., Alber, M., Hentschel, G., Newman, S. A., and Glazier, J. A., CompuCell, a multi-model framework for simulation of morphogenesis, Bioinformatics 20 (2004) 1129-1137.
3. Newman, S. A.. and Comper, W. D., 'Generic' physical mechanisms of morphogenesis and pattern formation, Development 110 (1990)1-18.
4. Hentschel, H. G. E., Glimm, T., Glazier, J. A., Newman, S. A., Dynamical mechanisms for skeletal pattern formation in the vertebrate limb, to appear in Proceedings R. Soc. Lond: Bio. Sciences (2004).
5. Murray, J. D., Mathematical Biology, Springer, Berlin, 2nd edition (1993).
6. Miura, T. and Shiota, K., Tgf Beta2 acts as an activator molecule in reaction-diffusion model and is involved in cell sorting phenomenon in mouse limb micromass culture, Dev. Dyn. 217 (2000) 241-249.
7. Moftah, M. Z., Downie, S., Bronstein, N., Mezentseva, N., Pu, J., Maher, P., Newman, S. A,, Ectodermal FGFs induce perinodular inhibition of limb chondrogenesis in vitro and in vivo via FGF receptor 2, Dev. Biol. 249 (2002) 270-282.
8. Tsonis, P. A., Del Rio-Tsonis, K., Millan, J. L., Wheelock, M. J., Expression of N-cadherin and alkaline phosphatase in the chick limb bud mesenchymal cells: Regulation by 1,25- dihydroxyvitamin D_3 and TGF-beta1, Exp. Cell Res. 213 (1994) 433- 437.
9. Steinberg, M. S., Reconstruction of tissues by dissociated cells, Science 141 (1963) 401-408.
10. Glazier, J. A. and Graner, F., A simulation of the differential adhesion driven rearrangement of biological cells, Phys. Rev. E 47 (1993) 2128-2154.
11. Upadhyaya, A., Thermodynamic and fluid properties of cells, tissues and membranes, Ph.D. thesis, University of Notre Dame (2000).
12. Turing, A. M., The chemical basis of morphogenesis, Phil. Trans. Roy. Soc. Lond. B 237 (1952) 37-72.
13. Alber, M., Glimm, T., Hentschel, H. G. E., Kazmierczak, B. and Newman, S. A., Stability of n-Dimensional Patterns in a Generalized Turing System: Implications for Biological Pattern Formation, submitted (2004)**.**
14. Zeng, W., Thomas, G. L., Newman, S. A., and Glazier, J. A., A Novel Mechanism for Mesenchymal Condensation during Limb Chondrogenesis in vitro, in Mathematical Modeling and Computing in Biology and Medicine: 5th Conference of the European Society of Mathematical and Theoretical Biology, Milan, V. Capasso and M. Ortisi (ed.) (2002).
15. Kiskowski, M. A., Alber, M. S., Thomas, G. L., Glazier, J. A., Bronstein, N. B., Pu, J., and Newman, S. A.. Interplay between activator-inhibitor coupling and cell-matrix adhesion in a cellular automaton model for chondrogenic patterning. Dev Biol 271 (2004) 372-87.
16. Cohen, M. M., Jr., and Kreiborg, S. Hands and feet in the Apert syndrome. Am J Med Genet 57 (1995) 82-96.
17. Alber, M., Kazmierczak, B., Hentshcel, H.G.E., Newman, S.A., Existence of solutions to a new model of avian limb formation, submitted (2004).
18. Martin, G. R. The roles of FGFs in the early development of vertebrate limbs. *Genes Dev* 12 (1998) 1571-86.